ChemPubSoc Europe

DOI: 10.1002/celc.201700653

CHEMELECTROCHEM Articles

Electrochemical Conversion of Carbon Dioxide into CHO-Containing Compounds on Multimetallic Porphyrins

Karla Calfumán,[a] Jessica Honores,[b] Diego Guzmán,[b] Macarena Ohlbaum,[b] Francisco Armijo,[b, c] Rodrigo Del Río,[b, c] and Mauricio Isaacs*[b, c]

This work describes the electrochemical reduction of carbon dioxide in aqueous solution mediated by tetraruthenated metalloporphyrins (TRP; Co(II) and Zn(II)) in Nafion (Nf) and polyvinyl chloride (PVC) as a support. The comparative aspects of the two polymeric matrices are expressed in terms of the electrocatalytic behavior toward carbon dioxide reduction of both sets of modified electrodes; values of overpotential and turnover frequency were calculated in each case. The modified electrodes under survey were able to reduce carbon dioxide at −600 mV vs Ag/AgCl showing an enhanced reduction current and a decrease in the required overpotential compared to a bare glassy carbon (GC) electrode. Potential-controlled electrolysis experiments were carried out at −1000 mV in order to compare the distribution of products. The production of formic acid, formaldehyde and methanol was confirmed at potentials where reduction of solvent may occur. Measurements of electrochemical impedance spectroscopy show the presence of one active site for GC/Nf/MTRP (where M = Zn(II) and Co(II)) and three for GC/PVC/MTRP. This information corroborates the high values of TOF obtained for GC/PVC/ZnTRP as the best electrocatalyst.

1. Introduction

Electrochemical reduction of carbon dioxide is of great significance for a neutral cycle of carbon to useful chemicals and materials. However, several drawbacks such as high overpotential, high applied voltage and high energy consumption exist in the course of the conventional electrochemical reduction process. Carbon dioxide is now known to be a major cause of global warming and the reduction of its atmospheric concentration has therefore become a critical issue.[1,2] Carbon dioxide conversion in chemical species containing C–H bonds is a highly desired process, mainly because these products can be transported and used with the same infrastructure already installed in most countries, hence, carbon dioxide can be recycled to generate a neutral cycle of carbon this idea has been considered the main 21th century challenge.[3,4]

The electrochemical reduction of CO_2 is a promising process for this aim; depending on the number of electrons transferred; it is possible to obtain several products, being the most interesting when two or more electrons are transferred producing formic acid or formaldehyde; or even better, generating methane, methanol or ethanol.[5–7] In order to obtain these products, electrocatalysts based on transition metals complexes containing multiple metal centers have been used to achieve multielectron transfer.[8,9] It has been demonstrated that the presence of a transition metal coordinated in the center of porphyrins along with the stabilization of its lower oxidation state, forming a M(I) species promotes coordination of CO_2 as axial ligand.[10,11]

One of the main drawbacks of the CO_2 reduction with metalloporphyrins is the generation of a bi-electron transfer to generate carbon monoxide (CO) as a reaction product; since carbon monoxide is a stable species, it may interrupt further electron transfer impeding the production of more reduced species such as CH_4, which would be potentially useful as a fuel.[10,11]

Recently, lower potential for CO_2 reduction has been obtained using cobalt protoporphyrin immobilized on a pyrolytic graphite electrode,[12] glassy carbon electrode modified with a cobalt(II) chlorin complex adsorbed on multi-walled carbon nanotubes[13] and the substitution of the four para-phenyl hydrogens of iron tetraphenylporphyrin by trimethylammonium groups,[14] moreover all of these complexes yield almost exclusively CO.

Tetraruthenated porphyrin (TRP) consists of a Tetrapyridylporphyrin (TPyP) coordinated with four Ru (II) complexes in the periphery of the macrocycle. These kind of macrocycles are particularly attractive because they display unusual electrocatalytic[15–17] and photoelectrochemical[18–20] properties. In particular, these porphyrins have been used in the electroanalytical detection of S (IV) oxoanions[21–23] and electrocatalytic reduction

[a] Dr. K. Calfumán
Departamento de Química
Universidad de Chile
Las Palmeras # 3415, Santiago
E-mail: karlacalfuman@gmail.com
[b] Dr. J. Honores, Dr. D. Guzmán, M. Ohlbaum, Dr. F. Armijo, Dr. R. Del Río, Dr. M. Isaacs
Departamento de Química Inorgánica
Pontificia Universidad Católica de Chile
Av. Vicuña Mackenna #4860, Santiago
[c] Dr. F. Armijo, Dr. R. Del Río, Dr. M. Isaacs
Centro de Investigación en Nanotecnología y Materiales Avanzados CIEN-UC
Pontificia Universidad Católica de Chile

Supporting information for this article is available on the WWW under https://doi.org/10.1002/celc.201700653

processes of O_2[24] and CO_2.[8,25] In all cases, a multielectron transfer is essential to enhance the catalytic activity.[4,8,21–23,26–28]

Polymers having good solubility along with lower gas permeability can also have attractive overall properties such as better optical clarity, superior mechanical properties, and high chemical/thermal stability. A strategy that may allow one to take full advantage of these is the use of polymers as support. Particularly in this case, the polymer acts as support of metalloporphyrins, substantially increasing reactivity and stability,[21,22,28] thereby optimizing the cooperative action between the metalloporphyrin molecule and the polymer by generating a 3D architecture.[21,22,27,28] The synergy between the metalloporphyrin and the polymer could find use in molecular electronics because it allows for both electronic and photonic conduction and also the development of anisotropic functional materials.[29] Also, important properties for clinical use, such as fluorescence and the photosensitive ability to generate singlet oxygen, which enables porphyrin to be used as an anticancer drug.[30,31] Moreover, a cobalt(II) porphyrin was successfully incorporated into polymer membranes for the optical sensing of imidazole and its derivatives.[32] Finally, metalloporphyrins (Fe, Co)-based conjugated porous polymer frameworks are new high-surface-area porous materials consisting of an extended conjugated skeleton and inherent mesoporous. These combinations have exhibited great potential in gas sorption/separation, catalysis and electrocatalysis such as oxygen,[33] dopamine,[34] hydrogen peroxide[28,35] among others.

The aim of this paper is the study of the electrochemical reduction of CO_2 in aqueous media on glassy carbon modified electrodes with tetraruthenated metalloporphyrins (M = Co (II) and Zn (II)) in Nafion and PVC as a support. The comparative aspects of the two polymeric matrices are expressed in terms of the electrocatalytic character of these modified electrodes such as overpotential and turn over frequency. Potential controlled electrolysis was carried out to determine the main soluble and gaseous reaction products and the selectivity obtained with each modified electrode.

In addition, AFM and electrochemical impedance spectroscopy measurements were carried out to characterize these modified electrodes in terms of morphology, viscoelastic and electrical properties respectively, elucidating aspects about their reactivity as a function of the electrical properties of the polymeric matrix.

2. Results and Discussion

2.1. Characterization of Modified Electrodes

Previous publications carried out by our research group describe the morphology of both surfaces modified electrode.[21,22,27] However, new insights and properties are described below.

GC/PVC/ZnTRP and GC/Nf/ZnTRP modified electrodes were morphologically characterized by atomic force microscopy (AFM). Figure 1 shows uniform topographies surfaces for both

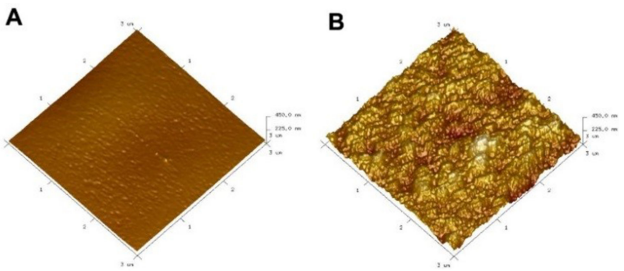

Figure 1. AFM images of A) GC/PVC/ZnTRP and B) GC/Nf/ZnTRP.

Table 1. AFM imaging characterization parameters.

Modified electrode	Properties [nm] Height	Roughness
GC	38.9	4.10
GC/Nf/ZnTRP	213.7	28.6
GC/Nf/CoTRP	438.5	63.8
GC/PVC/ZnTRP	45	7.15
GC/PVC/CoTRP	*	*

*Too fragile and thin film to be measured using this technique.

electrodes. Parameters such as height and roughness are summarized in Table 1.

Nafion modified electrodes have a roughness and height four times larger than those containing PVC. This could be caused by differences in the interaction between the porphyrin and Nafion or PVC. When using Nafion, two main interactions exist: an electrostatic interaction between the sulfonate groups found within the hydrophilic pores of the polyelectrolyte structure and the positive charges of MTRP, also a hydrophobic nature interaction, between the fluorocarbon chain of the Nafion and the π-system of the aromatic ring.[36] In addition, the bipyridine ligand allows for greater stacking between adjacent molecules.[37] In comparison, the only interaction between the PVC and the porphyrin is of hydrophobic nature, between the chlorocarbon chain of PVC and the π-system of the MTRP,[38] resulting in the incorporation of a smaller amount of porphyrin in the modified electrode.

AFM phase imaging characterization shows greater contrasts between GC/Nf/ZnTRP and GC/PVC/ZnTRP modified electrodes, as can be seen in Figure 2. These phase contrasts can relate to changes in the elastic and viscoelastic properties of different materials present on the analyzed surfaces.[39] GC/Nf/ZnTRP presents a uniformly heterogeneous surface (Figure 2B), allowed by the greater interaction and stacking between the Nafion and the porphyrin onto the modified electrode. On the other hand, GC/PVC/ZnTRP presents a lower phase (Figure 2A). It is possible to notice a non-uniform heterogeneous surface when a higher sensibility is used (Figure 2C), related to the lesser amount of PVC/ZnTRP incorporated onto the GC electrode. This can also be explained through the formation of nodules of irregular diameters of PVC polymer chains, which are randomly distributed on the modified electrode and trapped the ZnTRP through the previously mentioned hydrophobic interactions.[27] It should be

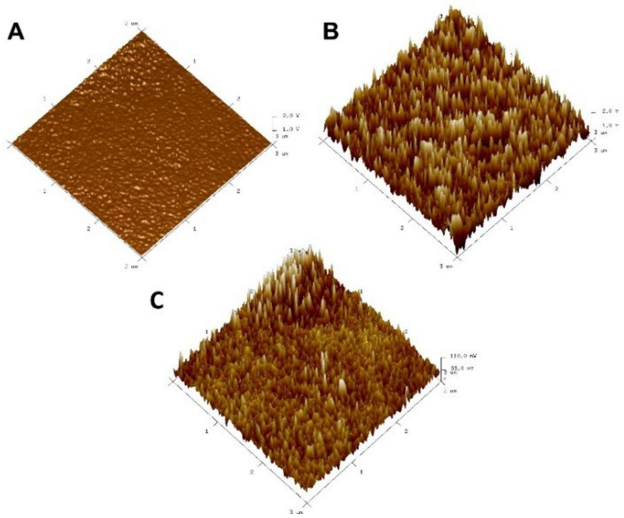

Figure 2. AFM phase imaging of A) GC/PVC/ZnTRP, B) GC/Nf/ZnTRP and C) expanded view of GC/PVC/ZnTRP.

noted that the modified electrodes with CoTRP exhibit similar behavior in Nafion matrix that the exhibited by ZnTRP (not shown). However, it was not possible to compare with its PVC analog due to manipulation problems of the film.

2.2. Voltammetric Studies of CO_2 Reduction

The electrocatalytic activity of GC, GC/Nf/MTRP and GC/PVC/MTRP was evaluated by comparing voltammetric response obtained in N_2 (pH = 6.1) and CO2 (pH = 4.2) gas atmosphere, under identical experimental conditions (see Figure 3). The inserts show the complete voltammetric profile of each modified electrode under N_2 atmosphere, porphyrin redox process associated with porphyrin is present at 0.8 V and corresponds to Ru(III)/Ru(II) redox couple.

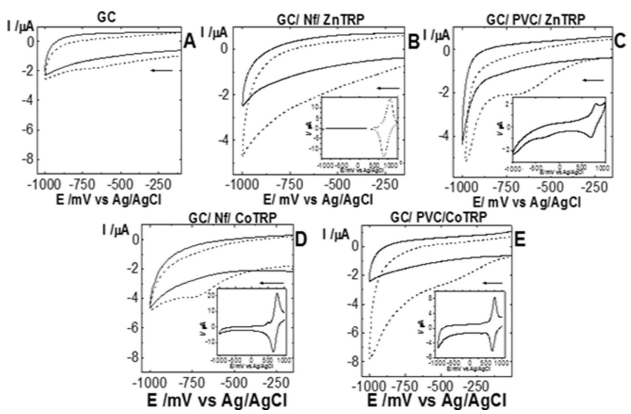

Figure 3. Voltammetric response of A) GC; B) GC/Nf/ZnTRP; C) GC/PVC/ZnTRP, D) GC/Nf/CoTRP and E) GC/PVC/CoTRP in 0.1 M $NaClO_4$, to 100 mV s^{-1} between 400 and −1000 V. Solid line: Without CO_2, dotted line: in presence of 32.9 mM CO_2 . Inset: Voltammetric profile modified electrode in 0.1 $NaClO_4$.

Considering our results and the information previously published;[40,41] it is possible to affirm that the Ru complexes in the periphery of the porphyrins act as electron reservoir where some molecular mechanism has been demonstrated; being the most likely retro-donation where electronic density is induced toward the metallic ion in the core of the macrocycle. For example the tetraelectronic reduction of O_2 to water.[24,42-47]

In the absence of CO_2, both glassy carbon and modified electrodes do not exhibit relevant voltammetric signals. However, when the solution is saturated with CO_2, there is a current increase possibly related to its reduction. Although the voltammetric wave associated with the reduction of CO_2 are not well defined, the current magnitude is greater than the value obtained with bare glassy carbon electrode, demonstrating that these electrodes reduce carbon dioxide in an electrocatalytic regime (See Figure 3).

These experimental results can be compared to existing literature reports, it could be found that the use of these modified electrodes decreases the overpotentials required to reduce CO2 in aqueous medium.

Electrocatalytic reduction of CO2 has been deeply studied in metal electrodes (Ag, In, Cu),[48–52] gas diffusion (Ag, Pb, Pt, Cu, Ru–Pd, Ag)[53–58] and in the presence of macrocyclic systems (porphyrins, phthalocyanines, tetrazamacrocycles, polypyridines).[59–62] In all cases high overpotentials are required to carry out the process, namely, between −1.0 and −2.5 V depending on experimental conditions (solvent, supporting electrolyte, temperature, pressure).

Comparing these data with the experimental results found herein, it is clear that the use of modified electrodes (GC/Nf/MTRP and GC/PVC/MTRP), decrease the overpotentials required to reduce CO_2 in aqueous medium and under ambient conditions of temperature and pressure.

2.3. Potential-Controlled Electrolysis and Product Analysis for the Electroreduction of CO_2

In order to evaluate the catalytic activity of the modified electrodes, as well as determining the reaction products, potential controlled electrolysis was carried out using GC, GC/Nf/CoTRP, GC/Nf/ZnTRP, GC/PVC/CoTRP and GC/PVC/ZnTRP as working electrodes.

Considering Ru(III)/(II) redox couple as reference pattern, a voltammetric profile of the modified electrodes before and after performing the electrolysis was recorded, in order to determine the stability of the modified surface during the experiment. After three hours of continuous electrolysis, all electrodes showed cyclic voltamograms similar to those registered before the electrolysis, in which the Ru(III)/Ru(II) redox couple remains detectable (not shown), confirming the presence of the electroactive species during the course of the experiment. However, it is possible to observe a slight decrease in their charge, fact that does not necessarily involve a loss of electroactive species. The loss of charge for all modified electrodes (obtained from Ru(III)/Ru(II) redox couple) after 3

electrolysis hours did not exceed 13% (see Table S1 in supporting information section).

Recent reports state that film morphology (monitored by AFM) is affected after being used as an electrocatalyst, suggesting mobility of the electroactive species on electrode surface that affects the morphology of the modified surfaces.[5,6]

TOF and faradaic efficiency obtained for each reaction products is presented in Table 2. From this table it is clear that

Table 2. TOF and Faradaic efficiency obtained for the reaction products.

Modified electrode	TOF [s^{-1}] (Faradaic Efficiency) HCOH	HCOOH	CH_3OH
GC/Nf/CoTRP	0.23 (64.1%)	0.03 (5.6%)	0.09 (8.4%)
GC/Nf/ZnTRP	0.37 (57.2%)	0.09 (4.4%)	0
GC/PVC/CoTRP	1.31 (21.2%)	0.04 (0.3%)	0
GC/PVC/ZnTRP		0	0.88 (25.7%)

no electrode is selective for a particular product, however all are active in the CO_2 reduction. Also, faradaic efficiency values do not sum 100%, meaning that missing species are produced which couldn't be identified nor quantified, being those in some cases the majority product.

According to the activity of the metal center present in the complexes, TOF value for GC/PVC/CoTRP is 44 times bigger than its analogue with Nf in case of formaldehyde, it is worth noting that there is also a production of formic acid in both matrices. On the other hand, it can be stated that electrodes that possess ZnTRP produce more CH_3OH among the modified electrodes studied in this work. In general, best catalytic results were obtained with PVC containing modified electrodes, on the other hand, Nafion modified electrodes produce more amount of product, but are less specific.

Electrocatalytic properties of the modified electrodes could be related to the presence of high electron density in the porphyrin ring, due to cooperative effects of the Ru complexes, this phenomenon transforms the active sites of the macromolecule into a Lewis base-like molecule that could trigger acid-base interactions. Thus, the reduced macrocycle could be able to attract acidic species such as H^+ and CO_2 (Lewis acid).[63,64] The selectivity of these catalysts seems to arise from the preferential reaction of the reduced intermediate species with CO_2 instead of H^+. This selectivity would also agree with the nature of the reduction product observed. Thus, if the catalyst in its reduced form reacts with CO_2 to form a complex M–CO_2, the subsequent protonation promotes the formation of a metallocarboxylic acid and a further reaction may produce CO by breaking a C–O bond to form hydroxide or water. Therefore, the reaction of the reduced form of the catalyst with CO_2 will lead to the formation of CO and if the electron transfer continues, it will produce HCOH. In contrast, if the catalyst in its reduced form reacts with protons in the first step to form an hydride complex and later, reaction of the hydrides with CO_2 will lead to the production of HCOOH.[65,66]

Koper et al.[67] recently published a theoretical study of the mechanism of the electrochemical reduction of CO_2 catalyzed by cobalt porphyrins. In their work, authors show that there are mainly two intermediaries to obtain HCOH as reaction product, those are [Eqs. (1), (2)]:

$$[Co(P)]^0 + CO_2 + H^+ + e^- \rightarrow [Co(P)\text{-}OCHO]^0 \quad (1)$$

$$[Co(P)\text{-}CO_2]^- + H^+ + e^- \rightarrow [Co(P)\text{-}OCHO]^- \quad (2)$$

Formation of (1) is thermodynamically difficult due to its high equilibrium potential (−0.92 V vs RHE), while (2) is kinetically slow due to switching of the binding mode of the CO_2 from C-bonded to O-bonded to form [Co(P)] but thermodynamically probable due to its equilibrium potential. Authors also show that HCOOH can be generated from hydrogenation or protonation of these intermediaries, however it is unlikely due to the negative potential at which the intermediary [Co(P)-OCH_2O] is formed (−1.79 V vs RHE), thus, the minority product.[67]

Koper results agree with our experimental evidence, since although the formation of the intermediate (2) is kinetically slow, electrolysis time used in our work may possibly be enough for its production.

On the other hand, production of CH_3OH is favored by decreasing the pH of the medium since two protons and two additional electrons are needed generate it from the intermediary adduct. In our case, this production is disfavored due to the basicity of medium.[68]

It is noteworthy that from the GC analysis no CO or H_2 were detected, and hence all the probable carbon monoxide species formed during the electrolysis experiment, may be consumed to generate other reaction products, acting as an intermediary.

Different values of TOF obtained (see Table 2) with the modified electrodes can be explained almost exclusively, as a function of the morphology that mainly leads directs the structure of the film. As mentioned,[27] modified electrodes with PVC show agglomerations of MTRP trapped between polymer chains, generating regular knots on the electrode surface. Thus, MTRP's will play a dual role in the electrode, in one hand acting as electrocatalysts and on the other, leading to an increase in the rugosity of the film.[27]

According to morphological characterizations registered for both set of modified electrodes, GC/PVC/MTRP film is much thinner than its Nafion analogue. Considering that reaction rate decreases significantly with increasing the thickness of the coating; rate of propagation of charge through thick films is much lower compared to thin or porous portions of material;[65] therefore there would be a faster electron transfer on the PVC system.

2.4. Electrochemical Impedance Spectroscopy (EIS)

Sharp et al. published the circuit describing the behavior of an electrode coated with a polymer, in this article an equivalent circuit is generated predicting the electrical properties of a modified electrode.[66] To understand the electroactive behavior of the modified electrodes electrochemical impedance measurements were carried out at −1 V in presence of N_2 and CO_2

respectively for GC/Nf/CoTRP and GC/PVC/CoTRP that were used as models. EIS experiments of CoTRP modified electrodes are shown in the following text, ZnTRP modified electrodes behave similar to CoTRP modified electrodes, and therefore their corresponding Nyquist and Bode plots are shown in supporting information (see Figure S1 and S2 in supporting information section).

Figure 4 shows the Nyquist and Bode plots for the GC/Nf/CoTRP modified electrode in presence of N_2 and CO_2 respectively. In Figure 4A (in presence of N_2), the Nyquist plot displays a small semicircle that can be seen in the high frequency region followed by Warburg behavior at the low frequency region. The same experiment is represented in Figure 4b through a Bode plot where a capacitive behavior can be observed at medium frequencies and a diffusional behavior at low frequencies corroborated by the 45° angle. Under a CO_2 atmosphere, it is possible to observe that the semicircle is now clear indicating a new electrodic process influenced by the presence of the substrate without a diffusional region. On the other hand, from Bode plot it is clear that the capacitive behavior is increased. From the analysis of circuit elements, it is possible to propose an equivalent circuit that is presented in Figure 5 and relevant data is summarized in Table 3. Experimental data was fitted with an error of 2%.[69]

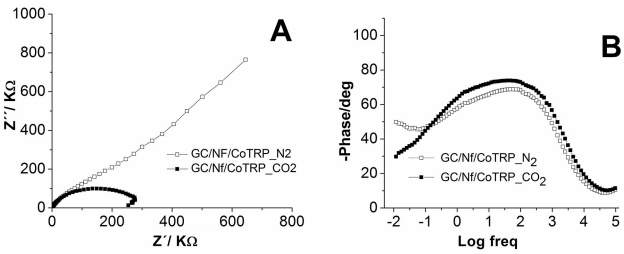

Figure 4. A) Nyquist and B) Bode plots of GC/Nf/CoTRP in the presence and absence of CO_2.

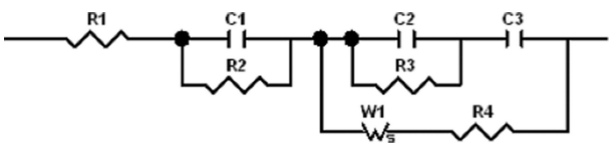

Figure 5. Equivalent circuit for the GC/Nf/CoTRP (χ^2 less than 0.001).

Where the first term (R1) on the left corresponds to the resistance of the solution between modified and reference electrode respectively; the R2 and C1 elements in series to R1 represent the interface film/solution where charge transfer across the film-solution phase boundary is required to maintain electroneutrality, a third sub-circuit which corresponds to the double layer capacitance (C3) at the electrode film-interface connected in series with a parallel combination of a capacitance C2 and a resistance R3 assigned to the dielectric properties of the bulk polymer; in parallel with the last, a resistance R4 (Rct) assigned to the heterogeneous electron transfer between the incorporated redox couple and the glassy carbon surface, in series with an impedance W1, which reflects limitation in the charge transport through the polymer bulk. Comparing N_2 and CO_2 atmospheres, the main significant parameters are C_2, R_3 and C_3, R_4, where the capacitances increase and the resistances decrease their values respectively. For the C_2 and R_3 case, it is possible to infer that dielectric properties of the polymer are affected by the presence of CO_2 when the electrocatalytic process mediated by CoTRP takes place as a local accumulation of charge due to the product formation. On the other hand, C_3 and R_4 are higher in absence of the catalytic process; in CO_2 atmosphere, it is evident since R_4 is one order of magnitude lower than N_2 atmosphere due to the generated reduction current. While C_3 under CO_2 is two orders of magnitude greater due to accumulation of protonated reaction intermediate or reaction products on the electrode/nafion interphase.

Table 3. The values of each element of the circuit (see Figure 5).

Element	Value GC/Nf/CoTRP in N_2	Value GC/Nf/CoTRP in CO_2
R1 [Ohm]	1.50×10^{2}	1.54×10^{2}
C1 [F g^{-1}]	2.96×10^{-8}	6.33×10^{-8}
R2 [Ohm]	8.21×10^{1}	4.19×10^{1}
C2 [F g^{-1}]	4.95×10^{-8}	2.52×10^{-7}
R3 [Ohm]	1.40×10^{6}	2.79×10^{5}
C3 [F g^{-1}]	2.44×10^{-7}	6.89×10^{-5}
W1-R [S sec^{-1}]	9.48×10^{8}	8.99×10^{7}
W1-T [S sec^{-1}]	6.58×10^{5}	5.83×10^{2}
W1-P [S sec^{-1}]	5.80×10^{-1}	7.30×10^{-1}
R4 [Ohm]	1.78×10^{3}	3.71×10^{2}

Figure 6 shows the Nyquist and Bode plots for the GC/PVC/CoTRP modified electrode in presence of N_2 and CO_2 respectively. Under N_2 atmosphere, Figure 6A, a small semicircle is observed at the high frequency region followed by a Warburg region. Under CO_2 atmosphere this behavior changes and the electrode resembles a capacitor in all the frequency region studied. This contrast is more evident if Bode plots are compared, Figure 6B, where under N_2 atmosphere three time constants are observed, however under CO_2 atmosphere a capacitive behavior is registered at a high frequency region and a diffusional process is revealed at low frequency region. From the analysis of circuit elements, it is possible to propose an

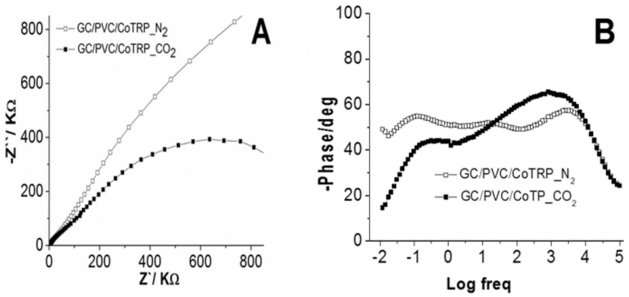

Figure 6. A) Nyquist and B) Bode plots of GC/PVC/CoTRP in presence and absence de CO_2.

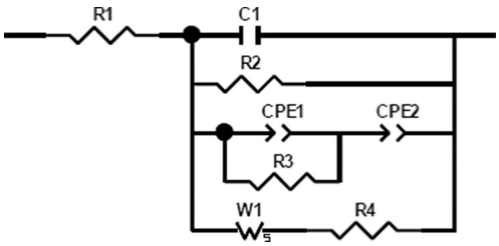

Figure 7. Equivalent circuit for the GC/PVC/CoTRP (χ^2 less than 0.001).

Table 4. The values of each element of the circuit (see Figure 7).

Element Value	GC/PVC/CoTRP in N_2	GC/PVC/CoTRP in CO_2
R1 [Ohm]	1.5×10^{-2}	1.5×10^{2}
C1 [F g^{-1}]	1.13×10^{-8}	1.26×10^{-8}
R2 [Ohm]	1.79×10^{7}	1.28×10^{6}
CPE1-T [F g^{-1}]	2.15×10^{-7}	1.12×10^{-6}
CPE1-P [F g^{-1}]	1.0×10^{0}	7.18×10^{-1}
R3 [Ohm]	9.52×10^{2}	6.25×10^{4}
CPE2-T [F g^{-1}]	2.65×10^{-6}	1.88×10^{-6}
CPE2-P [F g^{-1}]	5.98×10^{-1}	7.08×10^{-1}
W1-R [S sec^{-1}]	9.23×10^{13}	2.90×10^{13}
W1-T [S sec^{-1}]	1.11×10^{13}	4.83×10^{12}
W1-P [S sec^{-1}]	5.0×10^{-1}	5.0×10^{-1}
R4 [Ohm]	6.87×10^{6}	6.87×10^{6}

equivalent circuit which is presented in Figure 7 and relevant data is summarized in Table 4.

Comparing GC/Nf/CoTRP (Figure 5) and GC/PVC/CoTRP (Figure 7) it is possible to observe that circuit elements are almost the same, but connected in parallel in the last, except C_2 and C_3 that here appear as constant phase elements CPE_1 and CPE_2 respectively. The changes in the circuit are considerable, demonstrating the great effect of chemical composition of the membrane that supports the CoTRP electrocatalyst. This result is in accordance with morphology and viscoelastic properties observed in Figure 2. When the solution is saturated with CO_2, significant changes are observed CPE_1 and R_3; namely CPE_1 decrease in one order of magnitude from N_2 to CO_2 and R_3 decrease in three orders of magnitude form N_2 to CO_2. From these results, it can be inferred that the main process is corroborated in the inner structure of modified electrode, the resistance drops abruptly as a result of electron transfer reaction and subsequently the capacitance value decreases as a result of the release of intermediate protonated products from the hydrophobic domains present in PVC composite.

PVC containing electrodes presents non-uniform surface with variable rigidity zones (see point 3.1), resulting in high capacitances that compensate slow electrochemical reactions. Those capacitance values can be supplied by different elements of the circuit connected in parallel, each one with a different relaxation time τ ($\tau = RC$).[70] For the GC/Nf/CoTRP modified electrode a single τ is observed, while for GC/PVC/CoTRP three τ are clearly observable. This fact agrees with three different charge storage sites or in other words three active sites of reaction.

3. Conclusions

The carbon dioxide conversion to formaldehyde and others C–H–O compounds was performed by tetraruthenated metalloporphyrins (Co(II) and Zn(II)) in Nafion and PVC as a support.

Controlled potential electrolysis were carried out at −1000 mV; no evolution of H_2 is observed. Therefore, these modified electrodes verify the production of formic acid, formaldehyde and methanol at potentials where reduction of solvent is plausible demonstrating selectivity toward the carbon dioxide reduction.

TOF values obtained for GC/Nf/ZnTRP are in the order of 0.03 s^{-1}, while GC/PVC/ZnTRP approach the 1.63 s^{-1} (as function of HCOH production).

Measurements of electrochemical impedance corroborate and explain the high valuesof TOF obtained for the GC/PVC/MTRP vs GC/Nf/MTRP modified electrodes. Electrochemical impedance spectroscopy show that PVC electrodes presenting non-uniform surface with variable rigidity zones resulting in high capacitances that compensate slow electrochemical reactions. Those capacitance values can be supplied by three different relaxation times, this fact agrees with three different charge storage sites or, in other words, three active sites of reaction.

Considering the results obtained, the modified electrodes studied in this work can be good candidates to be components of Membrane Assembly Electrodes. The use of this kind of methodology would allow the carbon dioxide reduction in a continuous system.

Experimental Section

Reagents

All chemical reagents were of analytical grade or better. Cobalt (II) and Zn (II) acetate, 5,10,15,20 tetrapyridyl 21H, 23H porphine, tetrabutylammonium hexafluorophosphate ($TBAPF_6$), lithium trifluoromethanesulfonate (LiTFMS), polyvinyl chloride (PVC), dibutylftalate (DBP), sodium perchlorate and Nafion 117 were purchased from Sigma-Aldrich. Lithium chloride was purchased from Fisher Scientific.

Solvents Acetonitrile (ACN), Methanol, Tetrahydrofuran (THF), Acetone and Glacial Acetic Acid and neutral alumina were purchased from Merck. N_2 and CO_2 (extra pure, 99.995 %) were purchased from AGA-Chile.

The precursor complex cis dichloro (2,2′-bipyridine) ruthenium (II) dihydrate was prepared following the procedure described in the literature.[71] The complexes of Co (II), Ni (II) and Zn (II) μ-{*meso*-5,10,15,20-tetra(pyridyl)porphyrin} tetrakis{bis(bipyridine) (chloride) ruthenium(II)}$(PF_6)_4$ were prepared by the method described by Toma et al..[43,71–73] The purity of these compounds was checked by optical absorption spectroscopy, elemental analysis and ^{1}H-NMR.

Apparatus

Cyclic Voltammetry (CV) and electrolysis experiments were carried out using a CH-Instrument 620B potentiostat. Electrochemical Impedance Spectroscopy (EIS) measurements were carried out

using a CH-Instrument 760C bipotentiostat. UV-Visible measurements were performed in a Shimadzu Multispec 1501 spectrophotometer. Gas chromatography measurements (H_2, CO determination) were carried out by using a DANI MASTERS gas chromatograph: column: Supelco Mol sieve 5 Å (30 m × 0.53 mm) coupled with a microthermal conductivity detector (mTCD) by using argon as a gas carrier with an isothermal program (40 °C). Methanol content was determined by using a gas chromatograph coupled with a flame ionization detector (FID), with a Supelcowax 10 (30 m × 0.32 mm × 0.25 mm film thickness) column. AFM images were recorded on a Bruker NanoScope Innova AFM, along with NanoDrive v8.01 software. The images of the surfaces were investigated by using tapping and phase mode.

Cells, Electrodes and Procedures

Cyclic voltammetry and electrolysis experiments were performed in a Pyrex glass three electrode cell. Working electrodes were glassy carbon discs purchased from CH Instrument (r = 1.5 mm) in CV experiments, electrolysis experiments were carried out with a glassy carbon plate purchased from West Chester Pennsylvania (2.6 cm^2). A Pt wire (A = 8 cm^2) was used as auxiliary electrode, reference electrode was Ag/AgCl (sat) both from CH Instruments. After each experiment the GC electrode was polished with 0.3 μm alumina slurry, (Struers). The electrode was rinsed with double distilled, deionized water, cleaned in an ultrasonic water bath for 30 s to remove any remaining alumina, and then rinsed again with abundant deionized water.

The procedure for the preparation of the modified electrodes (ME) was done according to previously published articles.[21,27]

All the electrocatalytic measurements were carried out in aqueous solutions containing 0.1 M $NaClO_4$ (pH 6). For electrolysis experiments an H-type cell was used. The products were determined by quantitative colorimetric methods reported in the literature,[59,74] while for the gaseous products were analyzed by gas chromatography.

Controlled-Potential Electrolysis and Product Analysis

The potential was fixed at −1 V within 3 hours of experiment. Turnover frequency (TOF) was calculated as reported by Dreyse et al.[4] being moles of each product divided by moles of catalyst and time in seconds.

Under experimental conditions the main soluble products of CO_2 electroreduction were [Eqs. (3), (4), (5)]:

$$\text{Formic Acid}: \quad CO_2 + 2H^+ + 2\,e \rightarrow HCO_2H \tag{3}$$

$$\text{Formaldehyde}: \quad CO_2 + 4H^+ + 4\,e \rightarrow HCOH + H_2O \tag{4}$$

$$\text{Methanol}: \quad CO_2 + 6H^+ + 6\,e \rightarrow CH_3OH + H_2O \tag{5}$$

Formic acid and formaldehyde determination were performed using methods previously reported.[48,49] Finally for methanol determination gas chromatography was used (see 2.2 point). Concentration ranges and calibration curves are specified in supporting material section (see Table S2 and Figures S3–S5).

Electrochemical Impedance Spectroscopy Measurements

EIS measurements were carried out using glassy carbon and glassy carbon modified electrodes. All the measurements were carried out in presence of N_2 and CO_2 respectively at a working potential of −1 V vs Ag/AgCl, with amplitude of 5 mV, measured frequencies were from 10^{-3} Hz to 10^5 Hz. Experimental data obtained from the EIS measurements were fitted using CHI 760C software.

Acknowledgements

This work was supported by Nucleo Milenio CILIS-RC-130006, granted by Fondo de Innovación para la Competitividad, del Ministerio de Economía, Fomento y Turismo, Chile. K.C. acknowledges support from FONDECYT post-doctoral grant N°3150170. M.I. acknowledges support from FONDECYT project N°1141199.

Conflict of Interest

The authors declare no conflict of interest.

Keywords: carbon dioxide · electrocatalysis · electrochemical impedence · modified electrodes · porphyrins

[1] H. Zhao, Y. Zhang, B. Zhao, Y. Chang, Z. Li, *Environ. Sci. Technol.* **2012**, *46*, 5198–5204.
[2] C. B. Field, K. J. Mach, *Science* **2017**, *356*, 706–707.
[3] E. Barton Cole, P. S. Lakkaraju, D. M. Rampulla, A. J. Morris, E. Abelev, A. B. Bocarsly, *J. Am. Chem. Soc.* **2010**, *132*, 11539–11551.
[4] B. Chan, L. Radom, *J. Am. Chem. Soc.* **2006**, *128*, 5322–5323.
[5] P. Dreyse, J. Honores, D. Quezada, M. Isaacs, *Chem. Sus. Chem.* **2015**, *8*, 3897–3904.
[6] M. García, M. J. Aguirre, G. Canzi, C. P. Kubiak, M. Ohlbaum, M. Isaacs, *Electrochim. Acta* **2014**, *115*, 146–154.
[7] J. S. Yoo, R. Christensen, T. Vegge, J. K. Nørskov, F. Studt, *Chem. Sus. Chem.* **2016**, *9*, 358–363.
[8] J. Schneider, H. Jia, K. Kobiro, D. Cabelli, J. Muckerman, E. Fujita, *Energy Enviton. Sci.* **2012**, *5*, 9502–9510.
[9] Z. Y. Bian, K. Sumi, M. Furue, S. Sato, K. Koike, O. Ishitani, *Inorg. Chem.* **2008**, *47*, 10801–10803.
[10] C. Costentin, M. Robert, J. M. Saveant, *Chem. Soc. Rev.* **2013**, *42*, 2423–2436.
[11] J. D. Froehlich, C. P. Kubiak, *Inorg. Chem.* **2012**, *51*, 3932–3934.
[12] J. Shen, R. Kortlever, R. Kas, Y. Y. Birdja, O. Díaz-Morales, Y. Knon, I. Ledezma-Yanez, K. J. P. Schouten, G. Mul, M. T. T. Koper, *N, Commun.* **2015** doi:10.1038/ncomms9177.
[13] S. Aoi, K. Mase, K. Ohkubo, S. Fukuzumi, *Chem. Commun.* **2015**, *5*, 10226–10228.
[14] C. Costentin, M. Robert, J. M. Savéant, A. Tatin, *PNAS* **2015**, *22*, 6882–6886.
[15] C. Shi, F. C. Anson, *Inorg. Chem.* **1992**, *31*, 5078–5083.
[16] M. S. M. Quintino, K. Araki, H. E. Toma, L. Angnes, *Talanta* **2006**, *68*, 1281–1286.
[17] M. S. M. Quintino, H. Winnischofer, K. Araki, H. E. Toma, L. Angnes, *Analyst* **2005**, *130*, 221–226.
[18] A. Prodi, M. T. Indelli, C. J. Kleverlaan, E. Alessio, F. Scandola, A. Prodi, M. T. Indelli, C. J. Kleverlaan, E. Alessio, F. Scandola, *Coord. Chem. Rev.* **2002**, *229*, 51–58.
[19] M. R. Wasielewski, *Chem. Rev.* **1992**, *92*, 435–461.
[20] H. Winnischofer, A. L. Barboza Formiga, M. Nakamura, H. E. Toma, K. Araki, A. F. Nogueira, *Photochem. Photobiol. Sci.* **2005**, *4*, 359–366.
[21] K. Calfumán, M. J. Aguirre, D. Villagra, C. Yañez, C. Arévalo, B. Matsuhiro, M. Isaacs, *J. Solid State Electrochem.* **2010**, *14*, 1065–1072.
[22] K. Calfumán, M. García, M. J. Aguirre, B. Matsuhiro, L. Mendoza, M. Isaacs, *Electroanalysis* **2010**, *22*, 338–344.
[23] P. Dreyse, D. Quezada, J. Honores, M. J. Aguirre, L. Mendoza, B. Matsuhiro, D. Villagra, M. Isaacs, *Electroanalysis* **2012**, *24*, 1709–1718.
[24] F. C. Anson, C. Shi, B. Steiger, *Acc. Chem. Res.* **1997**, *30*, 437–444.
[25] K. Araki, H. Toma, *Luminescence, J. Photochem. Photobiol A.* **1994**, *83*, 245–250.

[26] P. Dreyse, M. Isaacs, K. Calfumán, C. Cáceres, A. Aliaga, M. J. Aguirre, D. Villagra, *Electrochim. Acta* **2011**, *56*, 5230–5237.
[27] K. Calfumán, P. Dreyse, C. Garcia, M. J. Aguirre, T. Beltran, E. Guillamón, I. Sorribes, C. Vicent, R. Llusar, M. Isaacs, *Macromol. Symp.* **2011**, *304*, 93–100.
[28] K. Calfumán, D. Quezada, M. Isaacs, S. Bollo, *Electroanalysis* **2015**, *27*, 2778–2784.
[29] K. Sugiyasu, S. Ogi, M. Takeuchi, *Polymer Journal* **2014**, *46*, 674–681.
[30] M. Moriishi, Y. Kitayama, T. Ooya, T. Takeuchi, *Langmuir* **2015**, *31*, 12903–12910.
[31] R. Xue, C. Ge, K. Richardson, A. Palmer, M. Viapiano, J. J. Lannutti, *ACS Appl. Mater. Interfaces* **2015**, *7*, 8606 – 8614.
[32] Y. Tan, N. Escorcia, A. Hyslop, E. Wang, Y. Tan, *Analytical Chemistry Research* **2015**, *3*, 70–76.
[33] G. Lu. Y. Zhu, K. Xu, Y. Jin, Z. J. Ren, Z. Liu, W. Zhang, *Nanoscale* **2015**, *7*, 18271–18277.
[34] X. Yan, Y. Gu, C. Li, L. Tang, B. Zheng, Y. Lu, Z. Zhang, M. Yang, *Biosens. Bioelectron.* **2016**, *77*, 1032–1038.
[35] Z. Wu, L. Chen, J. Liu, K. Parvez, H. Liang, J. Shu, H. Sachdev, R. Graf, X. Feng, K. Müllen, *Adv. Mater.* **2014**, *26*, 1450–1455.
[36] K. Calfumán, M. J. Aguirre, P. Cañete-Rosales, S. Bollo, R. Llusar, M. Isaacs, *Electrochim. Acta* **2011**, *56*, 8484–8491.
[37] J. C. Da Rocha, G. Dements, M. Bertotti, K. Araki, H. Toma, *J. Electroanal. Chem.* **2002**, *526*, 69–76.
[38] F. Zhao, J. Zhang, T. Abe, M. Kaneko, *J. Porphyrins Phthalocyanines* **1999**, *3*, 238–246.
[39] W. W. Scott, B. Bhushan, *Ultramicroscopy* **2003**, *97*, 151–169.
[40] K. Kuhl, E. Cave, D. Abram, T. Jaramillo, *Energy Environ. Sci.* **2012**, *5*, 7050.
[41] P. Dreyse, M. Isaacs, P. Iturriaga, D. Villagra, M. J. Aguirre, C. P. Kubiak, S. Glover, J. Goeltz, *J. Electroanal. Chem.* **2010**, *648*, 98.
[42] N4-Macrocyclic Metal Complexes, J. H. Zagal, F. Bedioudi, J. Dodelet (ed) 2006, Springer, USA.
[43] H. E. Toma, K. Araki, *Coord. Chem. Rev.* **2000**, *196*, 307.
[44] E. B. Fleischer. *Inorg. Chem.* **1962**, *1*, 493.
[45] J. Rochford, A. D. Rooney, M. T. Pryce, *Inog. Chem.* **2007**, *46*, 7247.
[46] S. F. Shkirman, K. N. Solo'ver, T. P. Kachura, S. A. Arabel, E. D. Skakovskil, *J. Appl. Spectroscopy* **1999**, *66*, 68.
[47] D. Mazaira, C. Borrás, J. Mostany, B. R. Scharifker, *J. of Electroanal. Chem.* **2009**, *631*, 22–28.
[48] B. Innocent, D. Liaigre, D. Pasquier, F. Ropital, J. M. Leger, K. B. Kokoh, *J. Appl. Electrochem.* **2009**, *39*, 227–232.
[49] K. Ohkawa, K. Hashimoto, A. Fujishima, Y. Noguchi, S. Nakayama, *J. Electroanal. Chem.* **1993**, *345*, 445–456.
[50] K. Ohkawa, Y. Noguchi, S. Nakayama, K. Hashimoto, A. Fujishima, *J. Electroanal. Chem.* **1994**, *367*, 165–173.
[51] M. Gattrell y N. Gupta, *J. Electroanal. Chem.* **2006**, *594*, 1–19.
[52] S. Kaneco, N Hiei, Y. Xing, H. Katsumata, H. Ohnishi, T. Suzuki, *Electrochim. Acta* **2002**, *48*, 51–55.
[53] M. N. Mahmood, D. Masheder, C. J. Harty, *J. Appl. Electrochem.* **1987**, *17*, 1159–1170.
[54] R. L. Cook R. L, R. C. MacDuff, A. F. Sammells, *J. Electrochem. Soc.* **1990**, *137*, 3309–3310.
[55] N. Furuya, T. Yamazaki, M. Shibata, *J. Electroanal. Chem.* **1997**, *431*, 39–41.
[56] K. Hara, T. Sakata, *J. Electrochem. Soc.* **1997**, *144*, 539–545.
[57] C. Sánchez-Sánchez, V. Montiel, D. Tryk, A. Aldaz, A. Fujishima, *Pure Appl. Chem.* **2001**, *20*, 1917–1927.
[58] K. Jeong, C. M. Miesse, J. Choi, J. Lee, J. Han, S. P. Yoon, S. W. Nam, T. Lim, T. G. Lee, *J. Power Sources* **2007**, *168*, 119–125.
[59] J. A. Ramos-Sende, C. R. Arana, L. Hernández, K. T. Potts, K. M. Keshevarz, H. D. Abruña, *Inorg. Chem.* **1995**, *34*, 3339–3348.
[60] N. Furuya, S. Koide, *Electrochim. Acta.* **1991**, *36*, 1309–1313.
[61] M. Isaacs, J. C. Canales, A. Riquelme, M. Lucero, M. J. Aguirre, J. Costamagna, *J. Coord. Chem.* **2003**, *56*, 1193–1201.
[62] P. A. Christensen, S. J. Higgins, *J. Electroanal. Chem.* **1995**, *387*, 127–132.
[63] J. Yun, F. Jun, A. Kishita, K. Tohji, H. Enomoto, *Journal of physics: Conference Series* **2010**, *215*, 012126.
[64] S. Fletcher, *J. Solid State Electrochem.* **2010**, *14*, 705–739.
[65] A. Bard, L. Faulkner, *Electrochemical methods: fundamentals and applications*, **2001**, Wiley, USA, pp. 580–628.
[66] M. Sharp, B. Lindholm-Sethson, E. Lotta-Lind, *J. Electroanal. Chem.*, **1993**, *345*, 223–242.
[67] J. Shen, M. J. Kolb, A. J. Göttle, M. T. M. Koper, *J. Phys. Chem. C.* **2016**, *120*, 15714–15721.
[68] J. Shen, R. Kortlever, R. Kas, Y. Y. Birdja, O. Díaz-Morales, Y. Kwon, I. Ledezma-Yanez, K. J. P. Schouten, G. Mul, M. T. M. Koper, *Nature Commun.* **2015**, DOI: 10.1038/ncomms9177.
[69] A. S. Sarac, M. Ates, B. Kilic, *Int. J. Electrochem. Sci.* **2008**, *3*, 777–786.
[70] M. Isaacs, F. Armijo, G. Ramírez, E. Trollund, S. R. Biaggio, J. Costamagna, M. J. Aguirre, *J. Mol. Cat.* A **2005**, *229*, 249–257.
[71] B. Sullivan, D. Salmon, T. Meyer, *Inorg. Chem* **1978**, *17*, 3334–3341.
[72] K. Araki, H. Toma, *J. Coord. Chem.* **1993**, *30*, 9–17.
[73] K. Araki, H. Toma, *J. Photochem. Photobiol.* **1994**, *83*, 245–250.
[74] C. E. Bricker, H. R. Johnson, *Ind. Eng. Chem.* **1945**, *17*, 399–402.

Manuscript received: June 30, 2017
Accepted Article published: September 22, 2017
Version of record online: October 18, 2017